

The background is a light beige color with a complex overlay of white and red line art. It includes molecular structures, a brain with neural connections, a hand holding a red tablet, and a cluster of hexagons containing medical icons like a heart, pills, and a microscope. The text 'HBV-TAG' is in a large, bold, dark red font, and '2021 CONFERENCE' is in a smaller, dark red font below it.

HBV-TAG

2021 CONFERENCE

The background is a solid reddish-orange color. Overlaid on this are several faint, white, semi-transparent graphics. On the left, a hand is shown holding a glowing orange DNA double helix. On the right, there is a cluster of hexagonal icons containing symbols for a clipboard, a heart rate monitor, a pill bottle, and a first aid kit. Faint network diagrams with nodes and lines are also visible across the background.

Molecular Genetics of HCC: When Should Tumor Genomic Sequencing be Done?

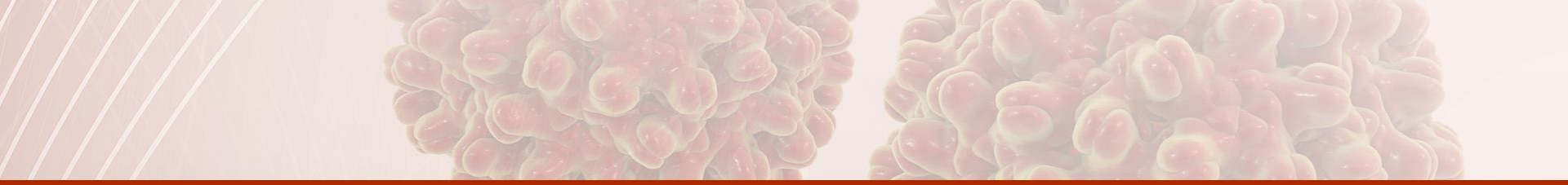
Lewis R. Roberts, MB ChB, PhD

Peter and Frances Georgeson Professor of
Gastroenterology Cancer Research, Mayo Clinic

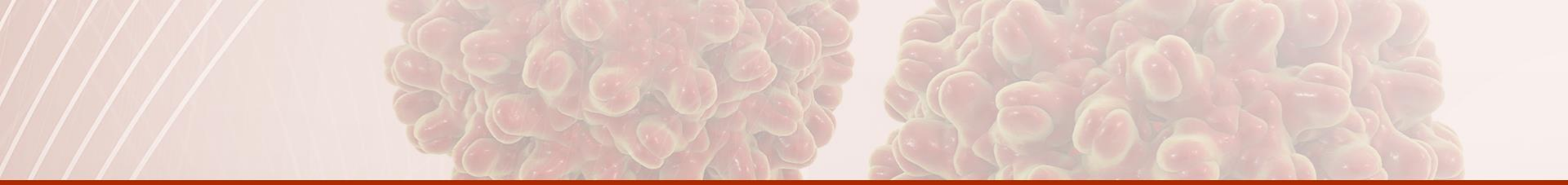
roberts.lewis@mayo.edu

Disclosures

- Ariad Pharmaceuticals – Grant Funding
- AstraZeneca – Advisory Board
- Bayer – Advisory Board, Grant Funding
- BTG International/Boston Scientific – Grant Funding
- Eisai – Advisory Board
- Exact Sciences – Advisory Board, Grant Funding
- Gilead Sciences – Advisory Board, Grant Funding
- Glycotest, Inc. – Grant Funding
- GRAIL, Inc. – Advisory Board
- QED Therapeutics, Inc. – Advisory Board
- RedHill – Grant Funding
- TARGET PharmaSolutions – Grant Funding
- TAVEC – Advisory Board
- Fujifilm Medical Systems – Grant Funding



And the Answer is:



And the Answer is: SOON!

CLINICAL CANCER RESEARCH

[Home](#)[About](#)[Articles](#)[For Authors](#)[Alerts](#)[News](#)[COVID-19](#)[Webinars](#)[Search Q](#)

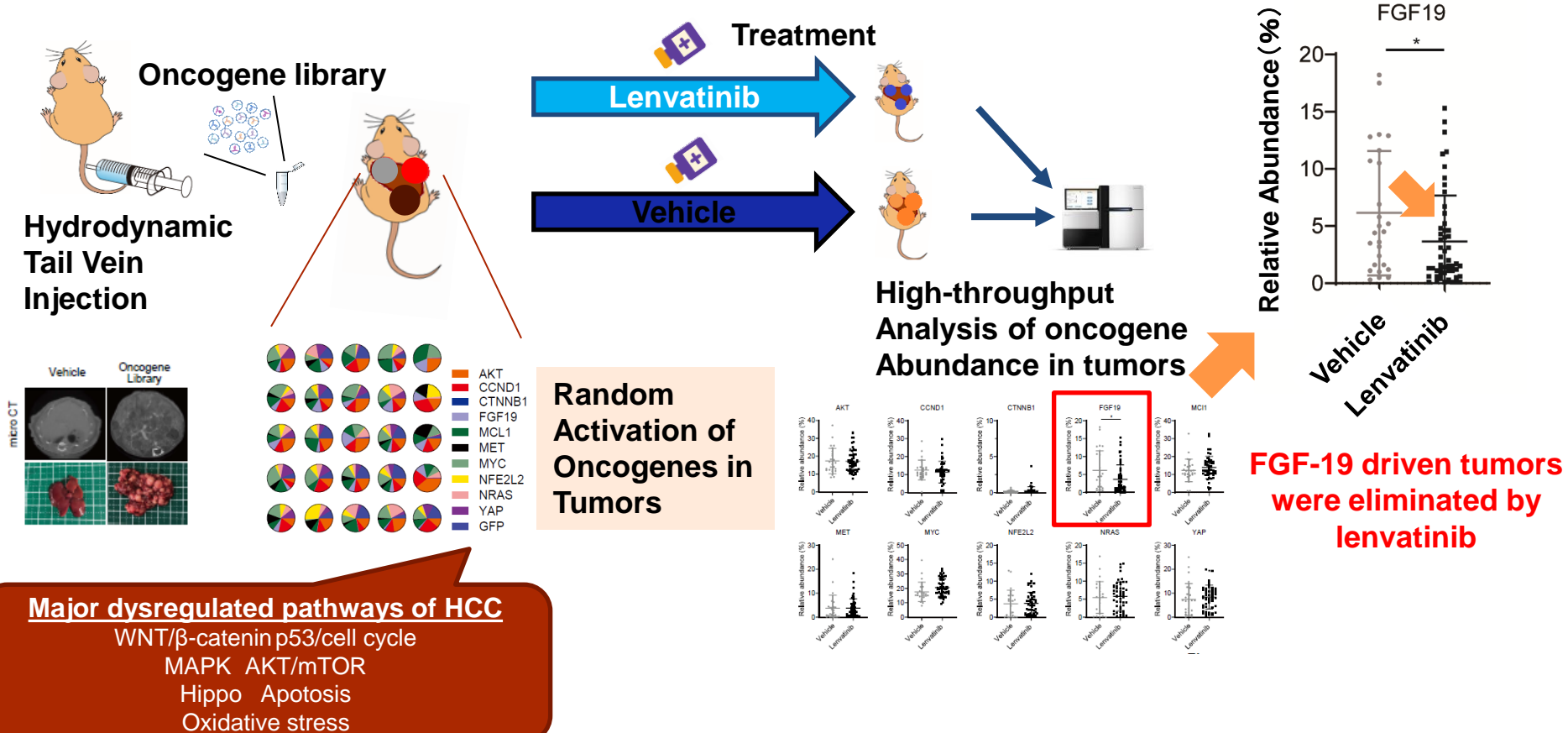
Translational Cancer Mechanisms and Therapy

ST6GAL1 Is a Novel Serum Biomarker for Lenvatinib-Susceptible FGF19-Driven Hepatocellular Carcinoma

Yuta Myojin, Takahiro Kodama, Kazuki Maesaka, Daisuke Motooka, Yu Sato, Satoshi Tanaka, Yuichi Abe, Kazuyoshi Ohkawa, Eiji Mita, Yoshito Hayashi, Hayato Hikita, Ryotaro Sakamori, Tomohide Tatsumi, Ayumu Taguchi, Hidetoshi Eguchi, and Tetsuo Takehara

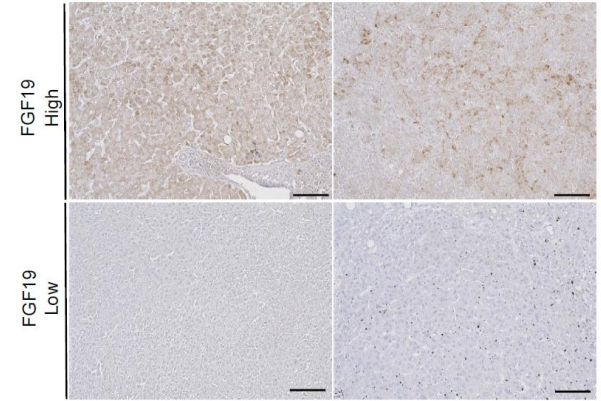
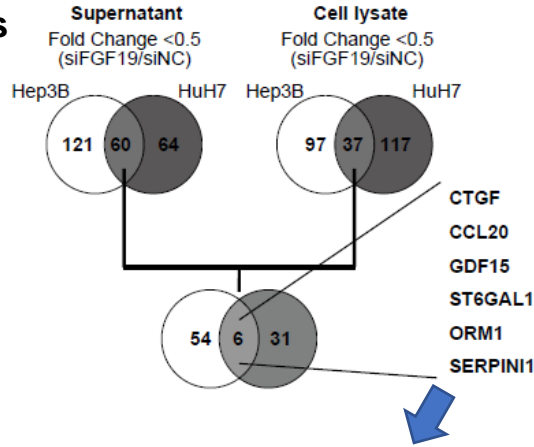
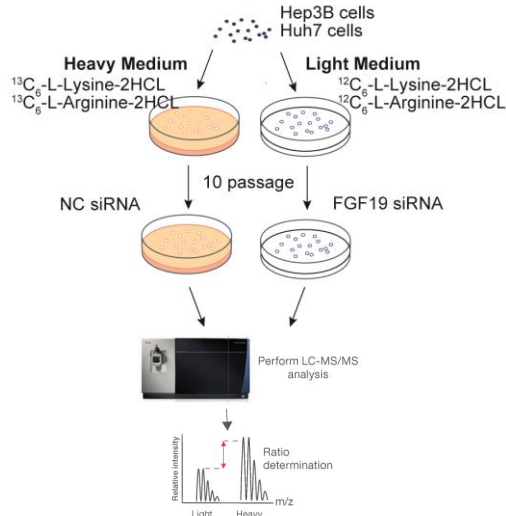
DOI: 10.1158/1078-0432.CCR-20-3382 Published February 2021 [Check for updates](#)

Liver tumor mouse model mimicking Inter-tumoral heterogeneity by introducing oncogene library

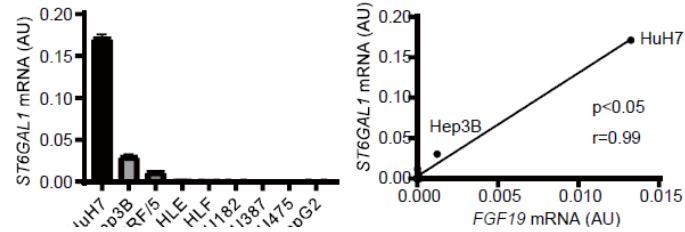


ST6GAL1 is identified as a serum protein positively regulated by FGF19 in HCC

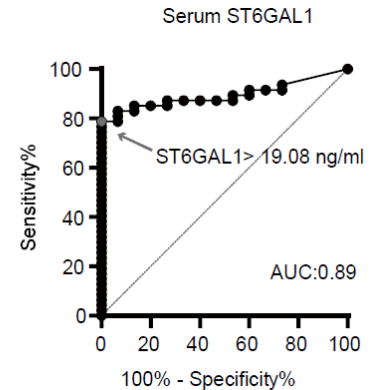
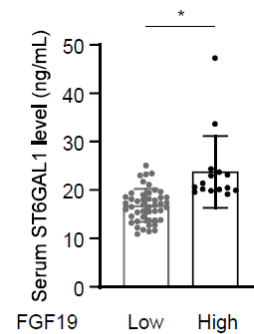
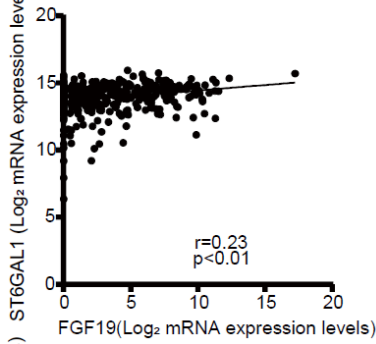
Proteome and Secretome analysis



HCC cell lines



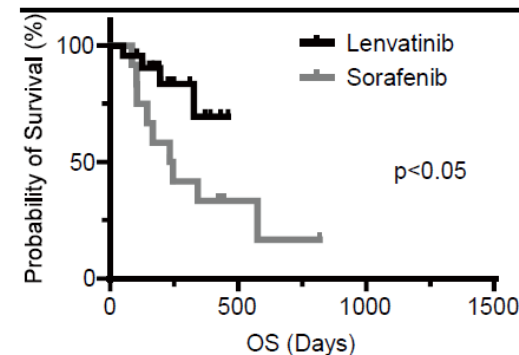
TCGA data base



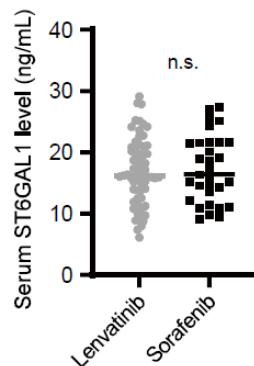
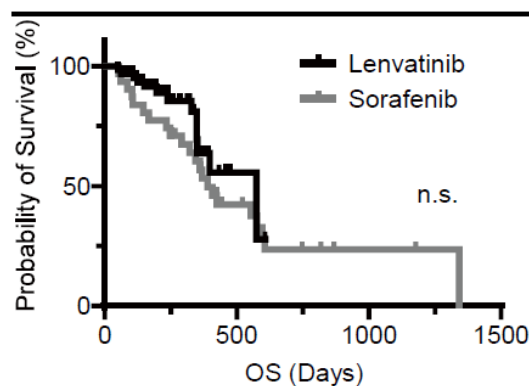
Serum ST6GAL1 is a biomarker of lenvatinib-susceptible HCC

Characteristics		Sorafenib Treatment (n = 31)	Lenvatinib Treatment (n = 65)	p value
Age (years)	Median (range)	70 (52-86)	73 (50- 89)	0.063
Sex, n (%)	Male / Female	25 (80.6) / 6 (19.4)	54 (83.1) / 11 (16.9)	0.77
Etiology, n (%)	HBV/HCV/NBNC	6 (19.4)/18 (58.1)/7 (2.5)	13 (20.0)/24 (36.9)/29 (44.6)*	0.23
Child-Pugh, n (%)	5/6/7/8	17(54.8)/ 5(16.1)/ 8(25.8)/ 1(3.3)	30 (46.1)/21 (32.3)/12 (18.5)/2 (3.1)	0.38
AFP (ng / mL)	Median (range)	29 (2-485968)	45.8 (1-33827)	0.96
Maximum tumor size (mm)	Median (range)	25 (9-100)	27 (1-330)	0.49
Tumor, n (%)	<7 / ≥7	12 (38.7) / 19 (61.3)	33 (50.8) / 32 (49.2)	0.27
BCLC stage	B / C	11 (35.5) / 20 (64.5)	36 (55.4) / 29 (44.6)	0.06

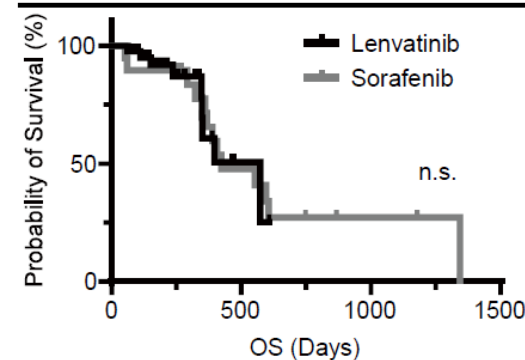
Serum ST6GAL1 High patients



All patients



Serum ST6GAL1 Low patients

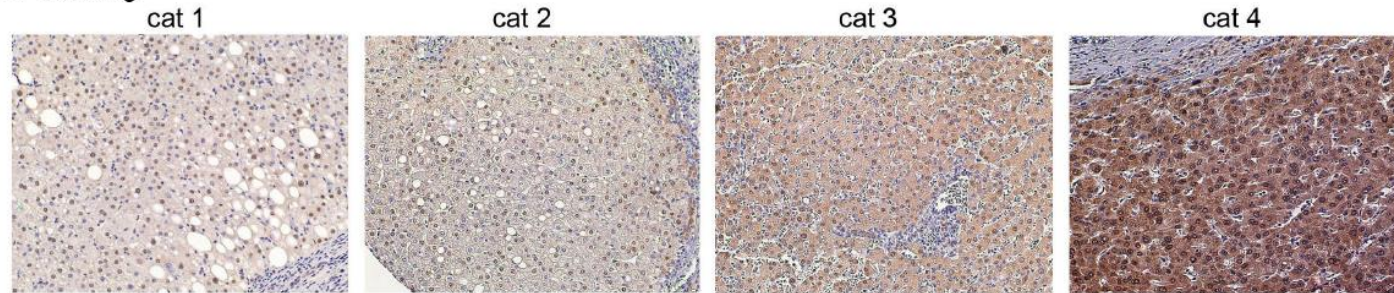


RNA Binding Protein APOBEC1 Complementation Factor (A1CF) Regulates Multiple Hepatic RNAs Promoting Steatosis, Fibrosis and Spontaneous Tumorigenesis

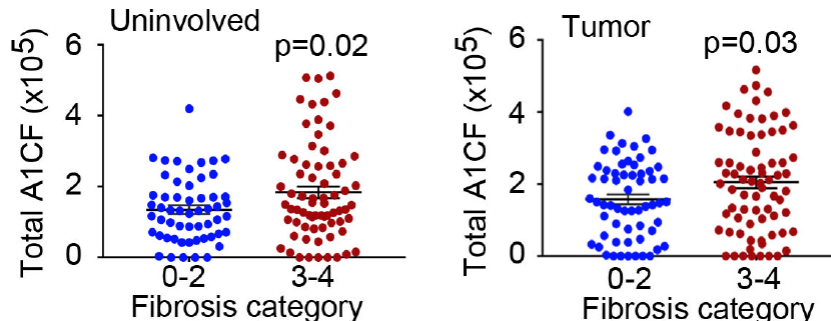
- RNA binding protein Apobec-1 Complementation Factor (A1CF) is expressed in human and mouse liver and binds ApoB mRNA, a gatekeeper gene regulating hepatic VLDL secretion. GWAS link A1CF with altered serum triglyceride and glycerol metabolism via mRNA splicing
- *A1cf*^{+Tg} mice show increased hepatic proliferation, spontaneous steatosis with decreased APOB and VLDL secretion
- Hepatic steatosis reflects increased lipogenic mRNA expression (Cd36, Cidea, Mogat1, Mogat2) and RNA shifts into polysome complexes
- Aged *A1cf*^{+Tg} mice showed fibrosis, spontaneous dysplasia and HCC (85%) which was accelerated by a high fat/fructose diet
- In TCGA 9% of 360 HCCs had aberrant A1CF expression and A1CF. In a human HCC TMA 35 of 137 (25%) had high levels of nuclear A1CF staining which correlated with stage 3/4 fibrosis and reduced overall and disease-free survival

High Nuclear A1CF Correlated with Stage 3-4 Fibrosis and Reduced Overall and Disease-Free Survival

A1CF staining

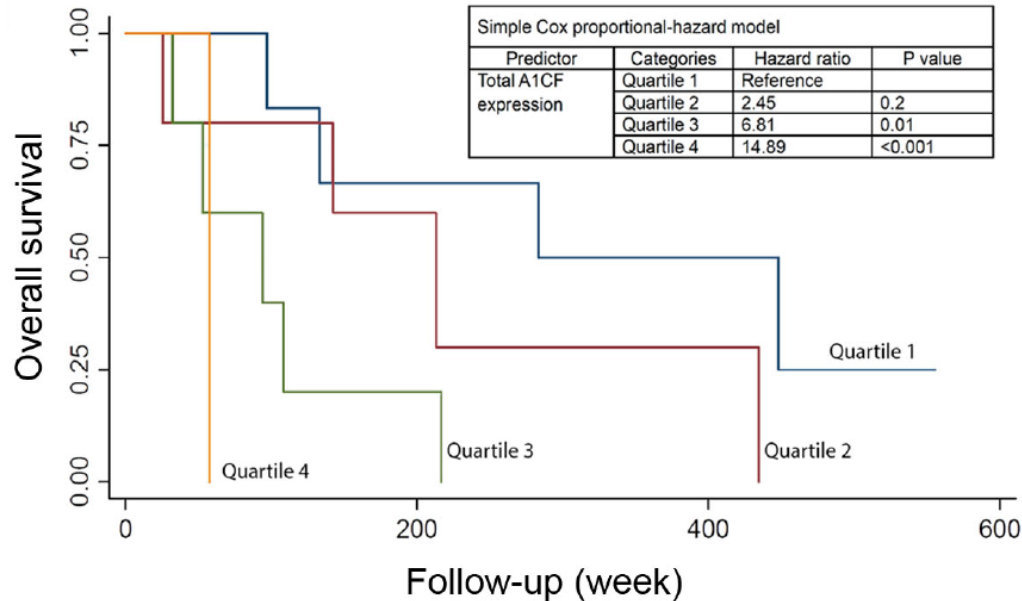


A1CF expression	Number of patients	
Category	Uninvolved	Tumor
1	39	36
2	45	36
3	23	30
4	20	35
Total	127	137



In a human HCC TMA 35 of 137 (25%) had high levels of nuclear A1CF staining which correlated with stage 3/4 fibrosis

High Nuclear A1CF Correlated with Stage 3-4 Fibrosis and Reduced Overall and Disease-Free Survival



High levels of nuclear A1CF staining correlated with reduced overall and disease-free survival.

This suggests that overexpression of A1CF impairs VLDL assembly and secretion, and promotes lipogenic and proliferative pathways resulting in spontaneous steatosis, inflammation and liver cancer in both mice and humans.

Hepatocellular cancer with concomitant Nrf2- β -catenin activation: Biological and therapeutic implications

Junyan Tao^{1,2}, Yaketrina Krutsenko^{1,2}, Sucha Singh^{1,2}, Aatur Singhi, Shuchang Liu^{1,2}, Satdarshan P. Monga^{1,2,3}

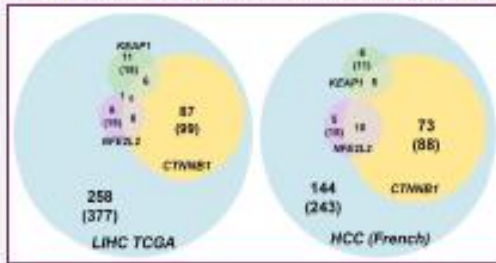
1. Department of Pathology,
2. Pittsburgh Liver Research Center, and
3. Department of Medicine, University of Pittsburgh, School of Medicine and University of Pittsburgh Medical Center, Pittsburgh, PA

Background and Methods

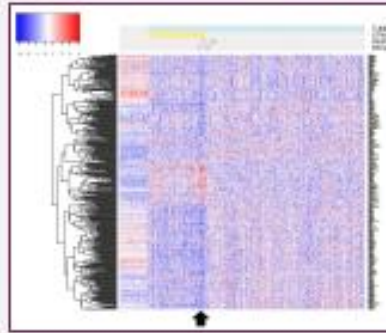
- Activating CTNNB1 mutations are seen in a subset of HCC
- β -catenin activation by itself is insufficient for hepatocarcinogenesis
- Co-expression of mutant CTNNB1 with clinically relevant co-occurrences leads to HCC
- Investigate cooperation between β -catenin and Nrf2 (encoded by NFE2L2) signaling
- HCC datasets assessed for presence of CTNNB1 mutations and either mutations in NFE2L2 or KEAP1 or Nrf2 activation by gene signature
- Sleeping beauty transposon/transposase hydrodynamic tail vein injection (SB HDTV)I
- T41A CTNNB1 co delivered with WT G31A or T80K NFE2L2 into 6 week old FVB mice
- Assessed for tumors and similarity to human HCC subsets by bioinformatics
- Given known mTORC1 activation in CTNNB1-mutated HCCs, response to monotherapy with the mTOR inhibitor everolimus was tested

~9% of Human HCCs Display CTNNB1 Mutations and NRF2 Activation

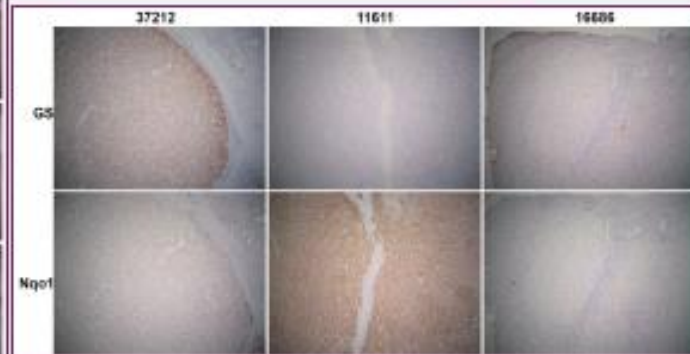
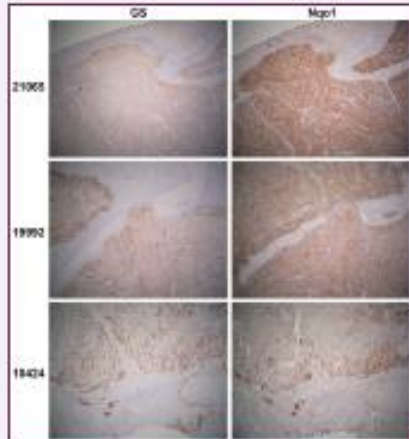
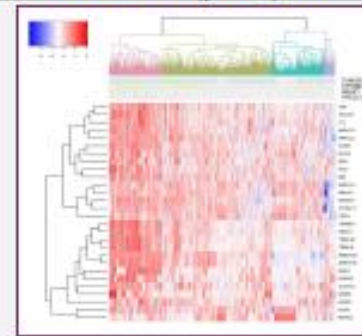
HCCs in TCGA & French cohort with overlap of CTNNB1 & NFE2L2/KEAP1 mutations



DEGs in dually mutated HCCs

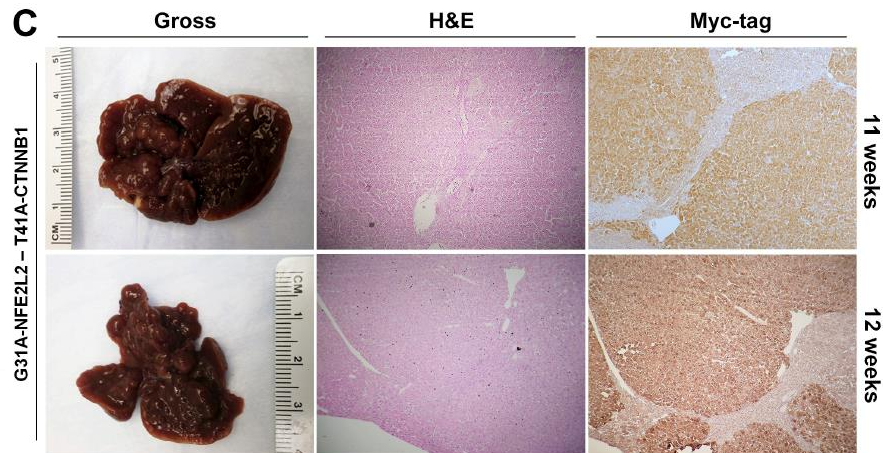
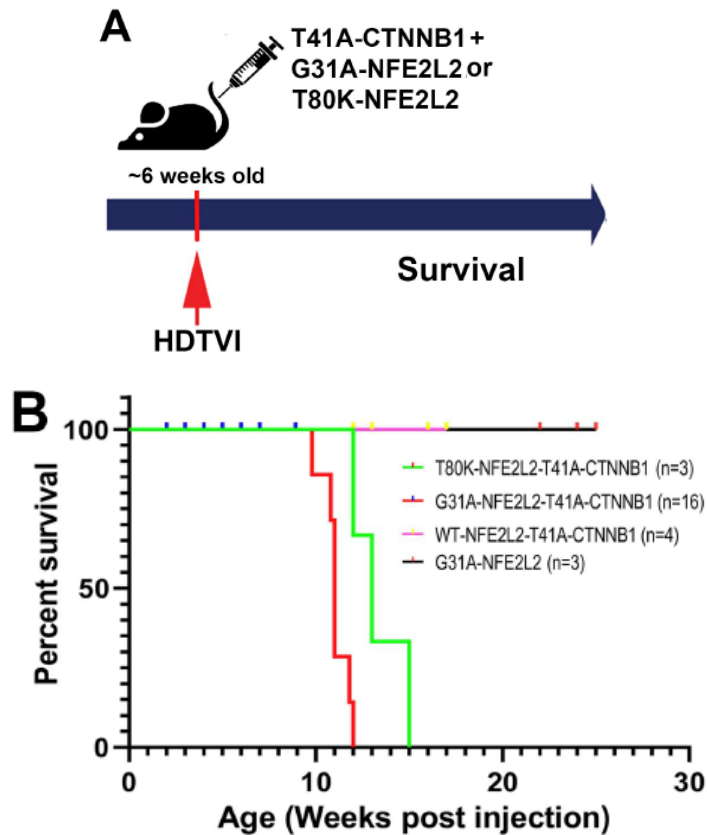


Concomitant Nrf2 activation (red) & CTNNB1 mutations (yellow) in 9% HCC

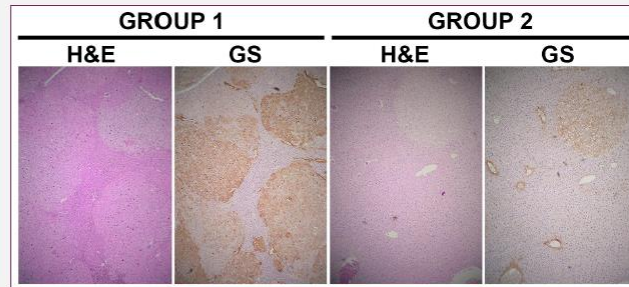
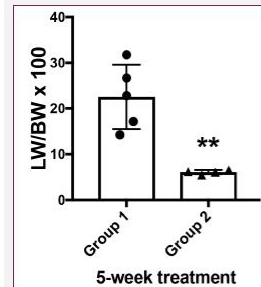
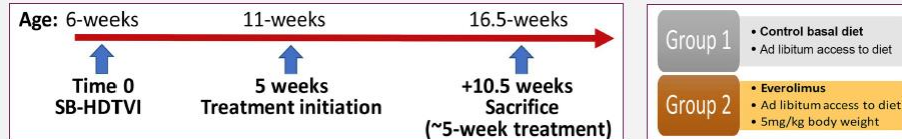
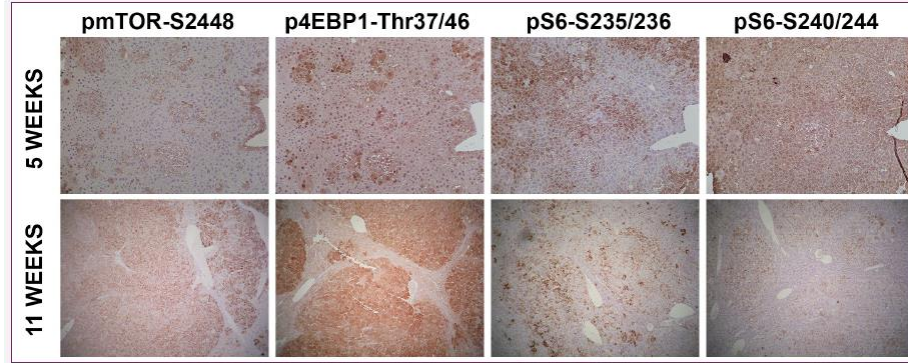


UPMC cohort shows around 12% of HCCs show co-expression of Nrf2 target Nqo1 & CTNNB1 target GS (left); Others showed discordance (right)

Co-expression of T41A CTNNB1 & G31A/T80K NFE2L2 but not WT NFE2L2 in liver by SB HDTV1 leads to HCC in mice



mTORC1 is active in β -catenin-Nrf2 HCC model & use of everolimus as monotherapy decreased tumor burden notably



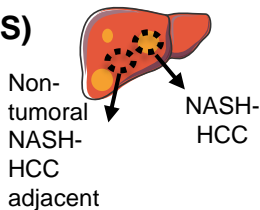
Molecular and mutational landscape of hepatocellular carcinoma (HCC) related to non-alcoholic steatohepatitis (NASH)

Marta Piqué-Gili, Roser Pinyol, Sara Torrecilla, Huan Wang, Carla Montironi, Pierluigi Ramadori, Catherine E. Willoughby, Carmen Andreu-Oller, Miguel Torres-Martin, Wei-Qiang Leow, Agrin Moeini, Patricia Taik, Judit Peix, Claudia PMS Oliveira, Venancio A. F. Alves, Anja Lachenmayer, Stephanie Roessler, Beatriz Minguez, Peter Schirmacher, Paolo Boffetta, Jean-Francois Dufour, Swan N. Thung, Helen Reeves, Andrew Uzilov, Flair J Carrilho, Charissa Y. Chang, Mathias Heikenwälder, Arun J Sanyal, Scott L. Friedman, Daniela Sia and Josep M Llovet

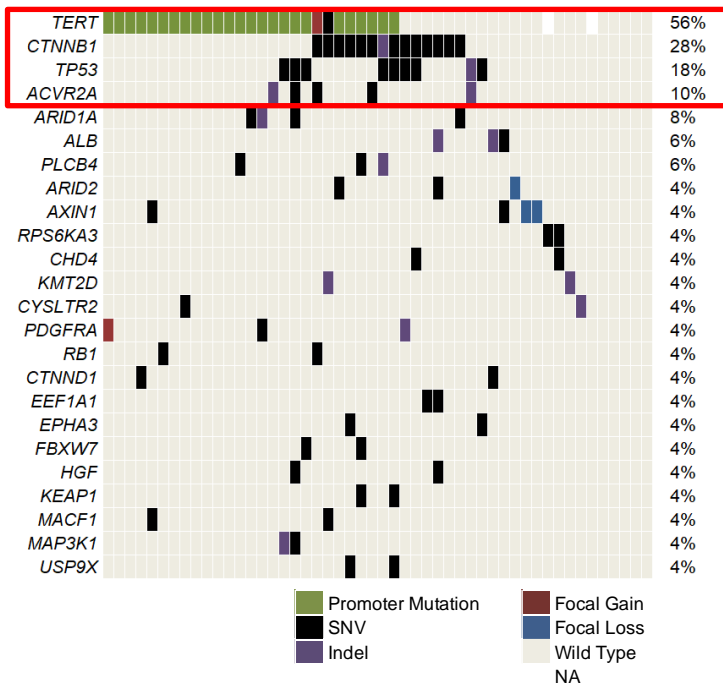
Genetic landscape of NASH-HCC

Whole Exome Sequencing (WES)

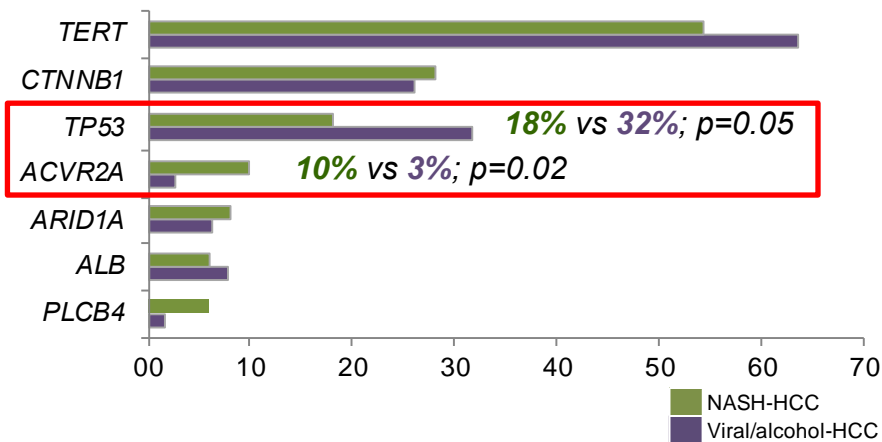
n=50 tumor-adjacent pairs



NASH-HCC:



NASH-HCC vs viral/alcohol-HCC (n=624):

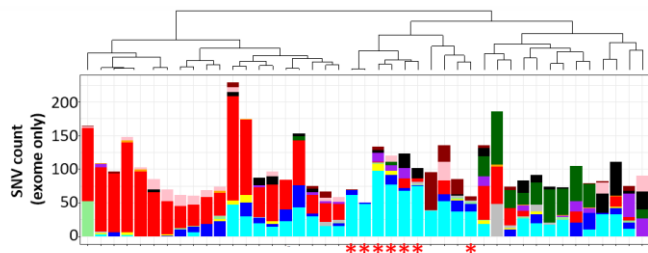


NASH-HCC patients presented higher **ACVR2A** mutations and a trend towards lower **TP53** mutation rates when compared to HCCs from other etiologies

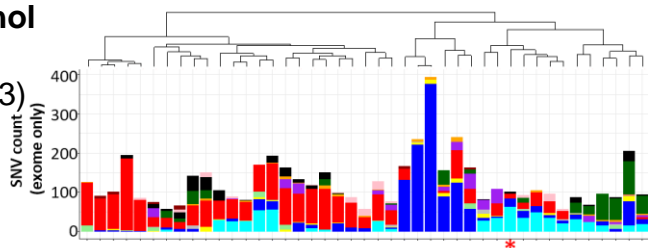
Mutational signatures in NASH-HCC and comparison with viral/alcohol-HCC

De novo mutational signature extraction

NASH-HCC
(n=43)



Viral/alcohol
-
HCC (n=43)



MutSig16

HCC: **19%** (16/86)

→ NASH-HCC: **19%** (n=8/43)

→ Viral/alcohol-HCC: **19%** (n=8/43)

Associated with larger tumors ($p < 0.05$)

MutSig24

HCC: **8%** (7/86)

→ NASH-HCC: **0%** (n=0/43)

→ Viral/alcohol-HCC: **16%** (n=7/43)

Associated with younger patients, vascular invasion and ↑ AFP ($p < 0.05$)

DenovoSig2

HCC: **9%** (8/86)

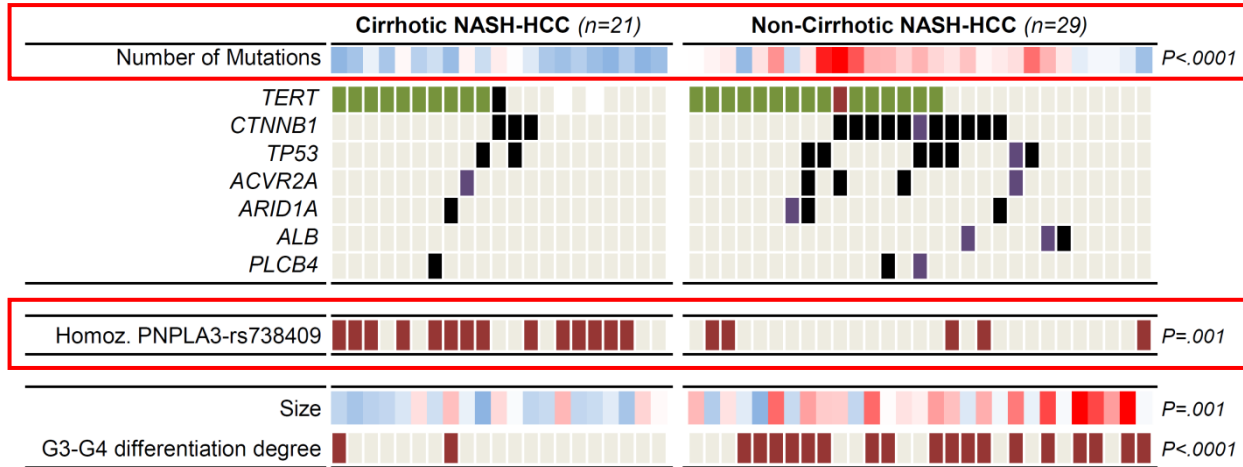
→ NASH-HCC: **16%** (n=7/43)

→ Viral/alcohol-HCC: **2%** (n=1/43)

MutSig-NASH-HCC

The newly-identified **MutSig-NASH-HCC** was associated with 16% of **NASH-HCC** tumors (vs 2% of HCCs from other etiologies)

Genetic landscape of NASH-HCC tumors according to cirrhotic status

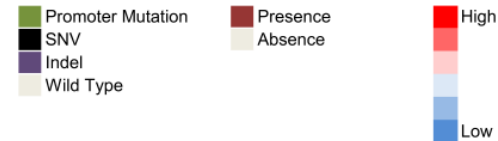


PNPLA3 SNP (GG)¹

↓ **mitochondrial function**
↓ **DNA repair response**

Non-cirrhotic NASH-HCC cases presented:

- ↑ **Tumor Mutational Burden** (1.45 vs. 0.94 mut/Mb, $p < 0.0017$)
- ↓ **Homozygous PNPLA3** (17 vs 67%, $p = 0.001$)



Key Takeaways

- NASH-HCC tumors present specific genomic features including high frequency of **ACVR2A** mutations (10%), low frequency of **TP53** mutations (18%) and the presence of the **MutSig-NASH-HCC**.
- **NASH** alone promotes a **cancer field** in **non-cirrhotic HCC** patients comparable to the one in **cirrhotic NASH-HCC**.

Overall, this study provides **novel insights** into the **NASH-HCC molecular pathogenesis** that may aid in the discovery of novel treatments for the disease and improve patient management

Article

NASH limits anti-tumour surveillance in immunotherapy-treated HCC

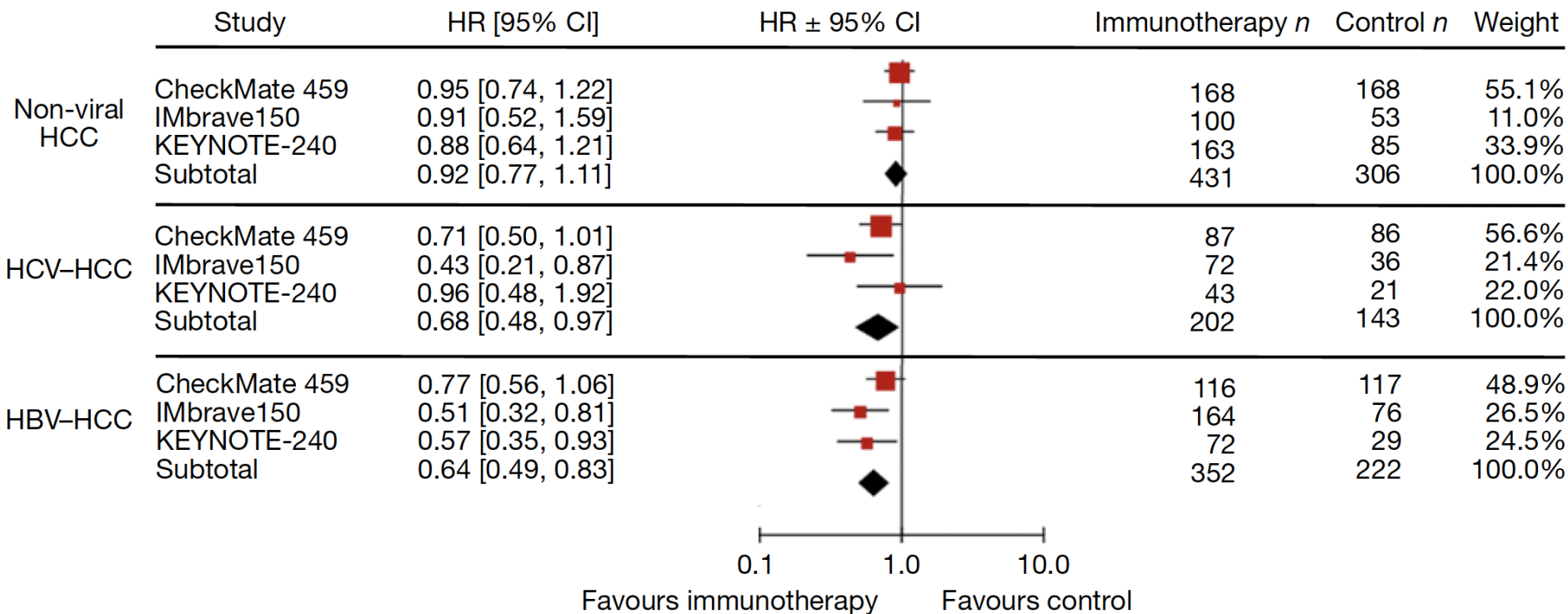
<https://doi.org/10.1038/s41586-021-03362-0>

Received: 17 February 2020

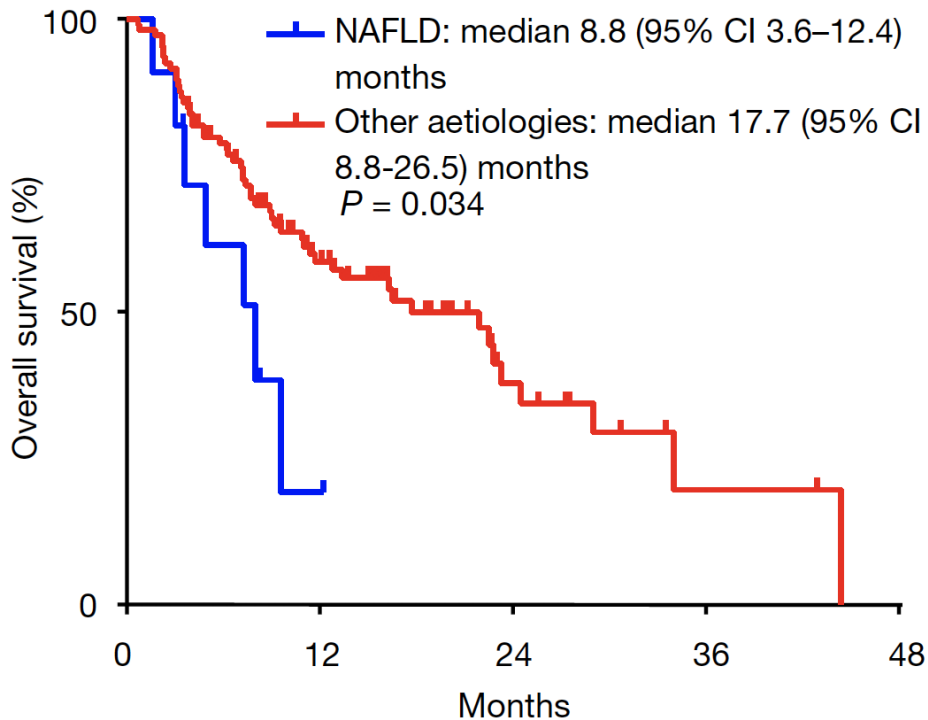
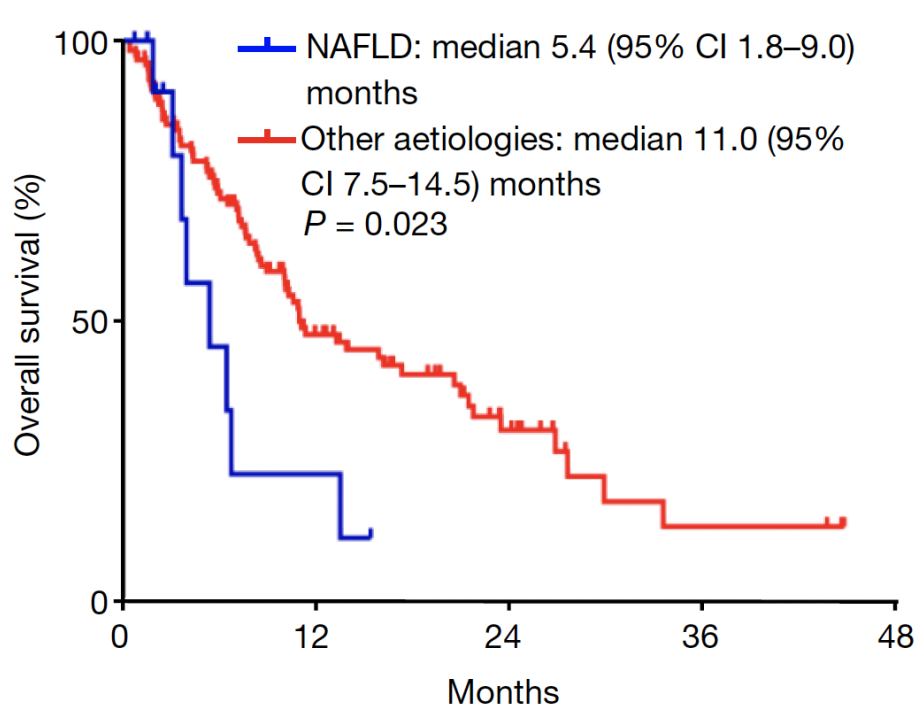
Accepted: 16 February 2021

Dominik Pfister^{1,82}, Nicolás Gonzalo Núñez², Roser Pinyol³, Olivier Govaere⁴, Matthias Pinter^{5,6}, Marta Szydłowska¹, Revant Gupta^{7,8}, Mengjie Qiu⁹, Aleksandra Deczkowska¹⁰, Assaf Weiner¹⁰, Florian Müller¹, Ankit Sinha^{11,12}, Ekaterina Friebel², Thomas Englertner^{13,14,15}, Daniela Lenggenhager¹⁶, Anja Moncsek¹⁷, Danijela Heide¹,

NASH HCCs are Resistant to Immune Checkpoint Inhibitors

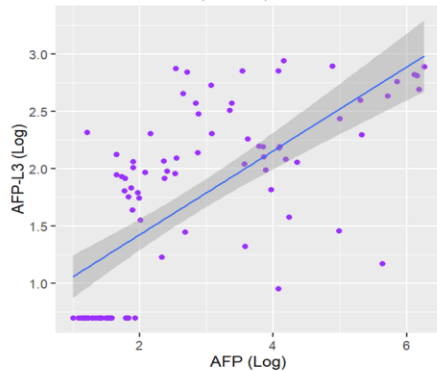


NASH HCCs are Resistant to Immune Checkpoint Inhibitors

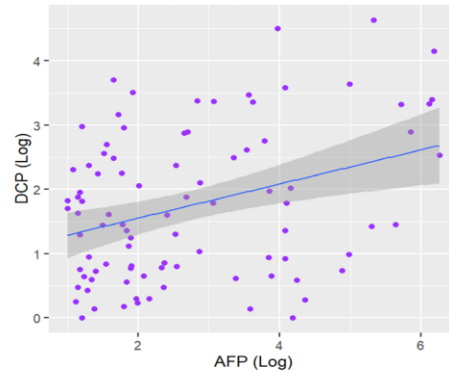


Genomic Associations of the GALAD Biomarkers

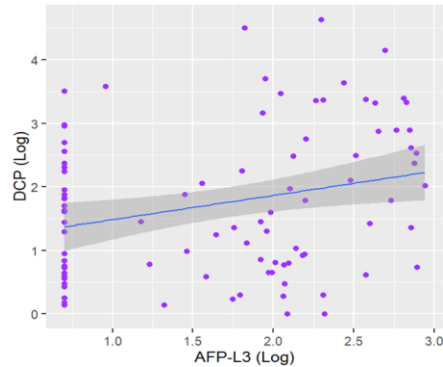
A AFP & AFP-L3 ($r=0.70$)



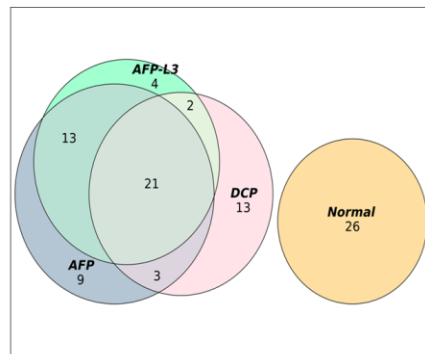
B AFP & DCP ($r=0.37$)



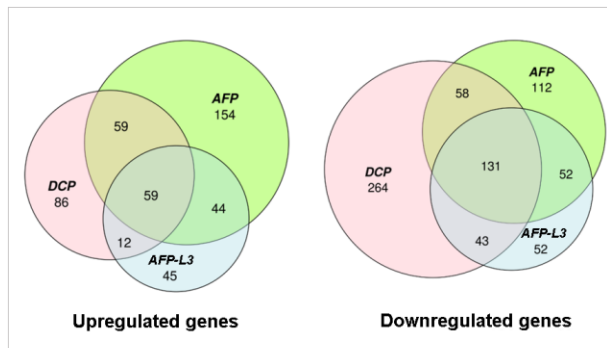
C AFP-L3 & DCP ($r=0.26$)



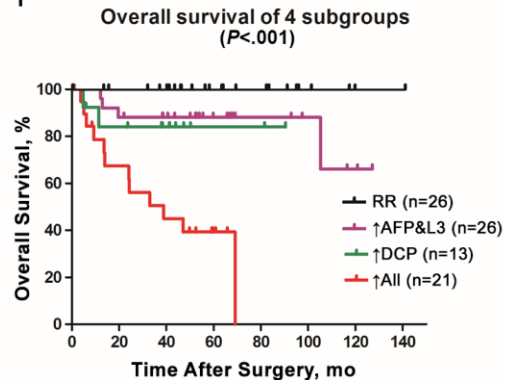
D



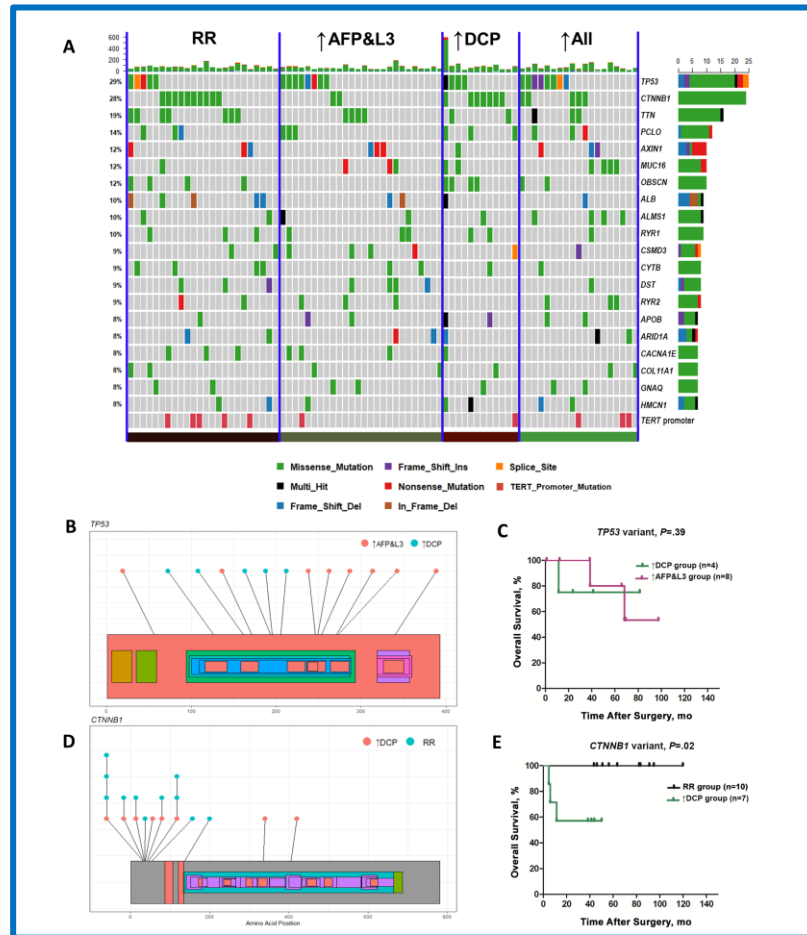
E



F



Genomic Associations of the GALAD Biomarkers

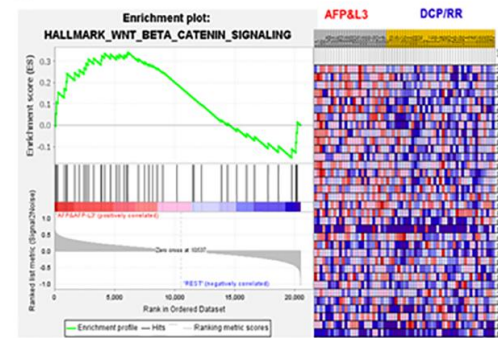


Genomic Associations of the GALAD Biomarkers

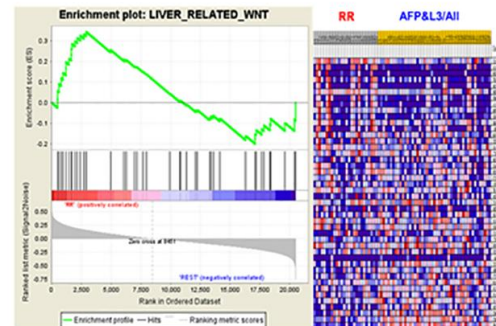
A

Pathway	RR	AFP&L3	DCP	All
NOTCH	Down	Up	Down	
p53			Down	
TGF- β		Up		
VEGF	Down	Up		Up
Wnt- β catenin	Down	Up		
Liver-related Wnt	Up			
IL6-JAK-STAT3		Up	Down	
MYC	Down	Up	Down	Up
PI3K-AKT-mTOR	Down	Up		Up
MAPK		Up		
Oxidative-phosphorylation	Up	Down	Down	
KRAS		Up	Down	Down

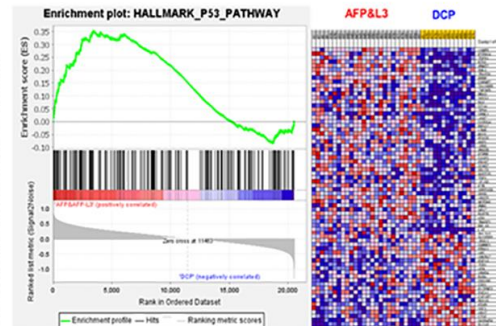
B



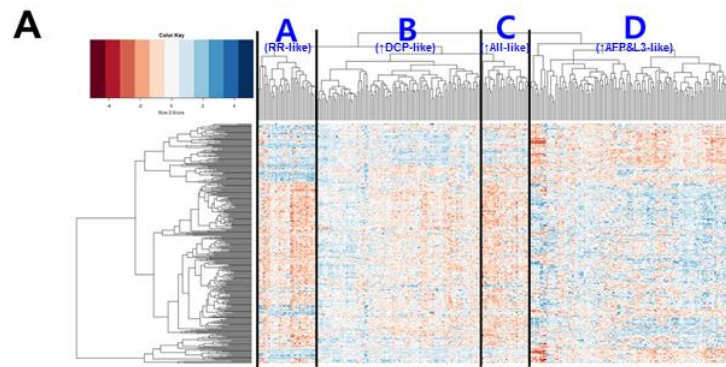
C



D

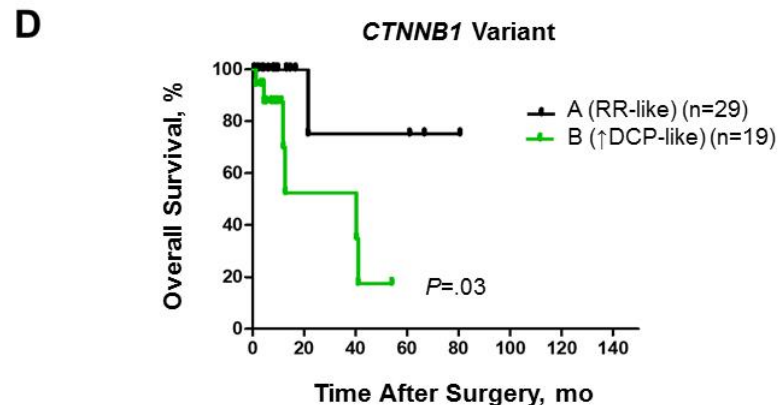
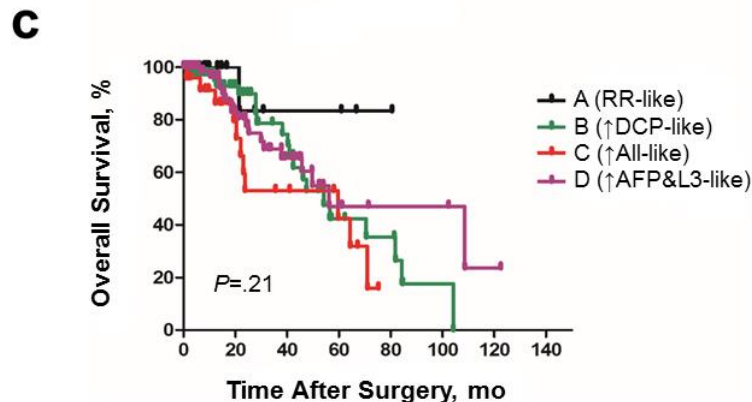


Genomic Associations of the GALAD Biomarkers



B

	A (RR-like) (n=35)	B (↑DCP-like) (n=97)	C (↑All-like) (n=28)	D (↑AFP&L3-like) (n=120)	P Value
Body mass index, mean (SD), kg/m ²	25.6 (5.1)	27.5 (7.0)	24.7 (4.0)	25.0 (6.6)	.048
Risk factor, No. (%)					.01
Alcohol	15 (45.5)	36 (37.9)	7 (25.9)	34 (30.9)	
Hepatitis B	5 (15.2)	11 (11.6)	5 (18.5)	19 (17.3)	
Hepatitis C	4 (12.1)	13 (13.7)	3 (11.1)	10 (9.1)	
Nonalcoholic fatty liver disease	0	6 (6.3)	0	0	
AFP(log), mean (SD)	0.9 (0.7)	1.1 (0.7)	1.6 (1.1)	2.4 (1.6)	<.001
TP53 variant, No. (%)	5 (14.3)	18 (18.6)	14 (50.0)	43 (35.8)	.001
CTNNB1 variant, No. (%)	29 (82.9)	19 (19.6)	3 (10.7)	12 (10.0)	.001



Genomic Associations of the GALAD Biomarkers

A

Biomarker Subgroup ^a	iClust 1 (n=65)	iClust 2 (n=55)	iClust 3 (n=63)
RR	1 (1.5%)	14 (25.5%)	13 (20.6%)
↑ AFP&L3	45 (69.2%)	8 (15.5%)	15 (23.8%)
↑ DCP	16 (24.6%)	25 (45.5%)	20 (31.7%)
↑ All	3 (4.6%)	8 (14.5%)	15 (23.8%)

^a $P < .001$

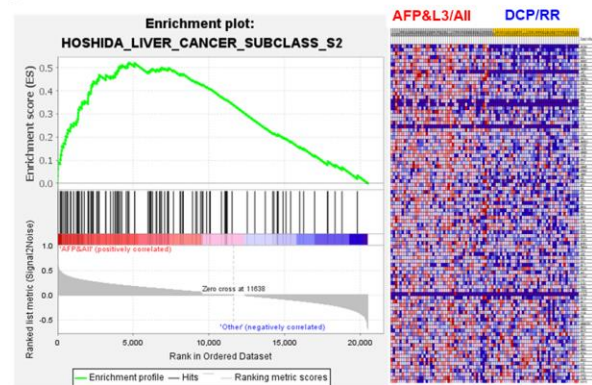
B

Hoshida Subclass	RR	↑ AFP&L3	↑ DCP	↑ All
S1	Down	Up	Down	Up
S2	Down	Up	Down	Up
S3	Up		Up	Down
Survival ^a	Up		Down	Down
Late recurrence ^b	Up		Down	Down

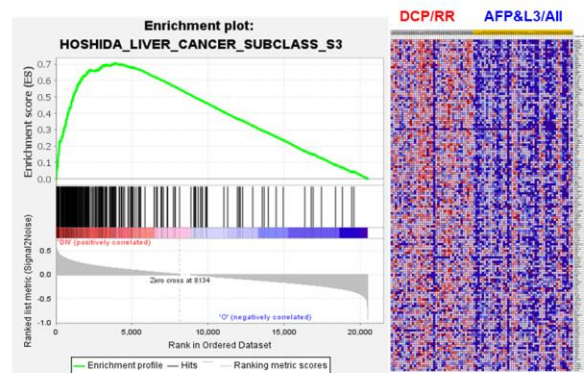
^a Genes whose expression correlated with good survival of HCC

^b Genes whose expression correlated with lower risk of late recurrence of HCC

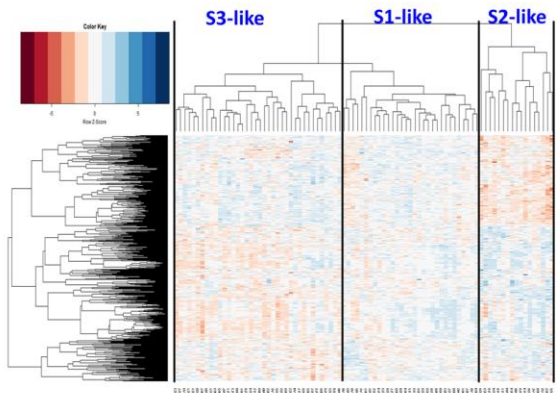
C



D



E



F

	S1-like (N=31)	S2-like (N=18)	S3-like (N=37)	P
Subgroups				<.001
RR	8 (25.8%)	1 (5.6%)	17 (45.9%)	
↑ AFP&L3	16 (51.6%)	6 (33.3%)	4 (10.8%)	
↑ DCP	2 (6.5%)	0 (0.0%)	11 (29.7%)	
↑ All	5 (16.1%)	11 (61.1%)	5 (13.5%)	
AFP (log, mean (SD))	2.8 (1.4)	4.2 (1.6)	2.0 (1.0)	<.001
AFP-L3 (log, mean (SD))	1.8 (0.7)	2.3 (0.6)	1.4 (0.8)	<.001
DCP (log, mean (SD))	1.3 (1.1)	2.2 (1.3)	1.6 (1.0)	0.05

Genomic Associations of the GALAD Biomarkers

Characteristics	↑AFP & L3	↑DCP	↑AFP&L3 + DCP	RR
Variant	<i>TP53</i>	<i>TP53</i> <i>CTNNB1</i> (Poor prognosis)	Heterogenous	<i>CTNNB1</i> (Good prognosis)
Molecular Pathways	WNT, TGB-beta, Notch VEGF, PI3K-AKT-mTOR, MYC, KRAS	Metabolism P53	MYC, PI3K-AKT-mROT, VEGF, metabolism	Liver-related WNT metabolism
Clinical phenotypes	Hepatitis B Moderate survival	Fatty liver, alcohol Moderate survival	Mixed risk factors Poorly differentiated Large tumor Poor survival	Fatty liver, alcohol Well differentiated Good survival
Published subclass (TCGA-LIHC, Hoshida)	iClust 1 S1, 2 (low risk)	iClust2 S3 (high risk)	S2 (high risk)	iClust 2 S3 (low risk)

Thank You!